Preprint
UCRL-JC-141033

Thermal Cavity Problem

P. M. Gresho, S. Sutton

This article was submitted to
Massachusetts Institute of Technology on Computational Fluid and Solid Mechanics
Cambridge, MA

October 11, 2000

U.S. Department of Energy

Lawrence
Livermore
National
Laboratory

8:1 Thermal Cavity Problem

P. M. Gresho and S. Sutton

Lawrence Livermore National Laboratory, Livermore, CA 94550, USA

Abstract

We present results for the 8:1 thermal cavity problem(1) using FIDAP on 3 meshes—each using 3 elements. A brief summary of related results is also included.

Keywords: Finite elements, FIDAP, thermal convection, CFD

1. Introduction

This contribution comes via the rather versatile and general commercial finite element code, FIDAP(2). This code still offers the user a wide selection with respect to element choices, statement of governing equations, (e.g., advective form, divergence form) implicit time integrators (variable-step or fixed step, first-order or second-order), and solution techniques for both the nonlinear and linear sets of equations. We have tested quite a number of these variations on this problem; here we report on an interesting subset and will present the remainder at the conference.

2. Methodology

Most of the results were obtained using the classical "plane vanilla" (and less expensive) Galerkin finite element method—no tricks, such as stability-enhancing upwind-related modifications to the advection terms—combined with an 'honest' non-dissipative second-order accurate time integrator: trapezoid rule(3) (TR). However, to demonstrate the often-deleterious effects of "stabilizing" modifications, we shall present some SUPG (Streamline-Upwind Petrov-Galerkin) results as well one from a highly-dissipative time integrator: backward Euler (BE).

In the results to be summarized herein, two types of solvers were employed on the linear systems resulting after the successive substitution (Picard) method was applied to each nonlinear algebraic system: (1) After applying the penalty approximation method to eliminate the pressure ($P= -\lambda\nabla.\mathbf{u},$), the *fully-coupled* ($\mathbf{u}$, Θ) systems were solved using an efficient form of Gaussian elimination (skyline method [2,3]). (2) The segregated solution method [2,3] was employed to generate an iterative sequence of smaller (uncoupled) linear systems (for u, v, Θ & P, as well as one for a Lagrange multiplier), each of which is solved by an iterative method. The symmetric systems (P and the Lagrange multiplier) were solved using the SSOR-preconditioned CR (conjugate residual) method and the unsymmetrical ones (u, v, Θ) via CGS (conjugate gradient squared), preconditioned with diagonal (Jacobi) scaling. Convergence criteria employed were as follows: $\varepsilon_N = 10^{-7}$ for the outer (Picard) iterations and $\varepsilon_L = 10^{-4}$ for the linear subsystems. The outer iterations typically converged in 3 - 5 iterations and the linear subsystems required 2-6 via CGS & 20-80 via CR. Sufficient testing assured us that our ε's were sufficiently small—via both relative error and relative residual (Euclidean) norms; i.e., $||\Delta x||/||x|| < \varepsilon$ and $||R(x)||/||R(x_o)|| < \varepsilon$, where $R(x) \equiv Ax-b$.

3. Results

In this 'short' presentation, we will show results from 3 elements on 3 grids—most via TR but with one using BE. The elements used were: (1) Q_1Q_0 (bilinear velocity and temperature, piecewise-constant pressure on Quadrilaterals), (2) Q_2P_{-1} (biquadratic velocity and temperature, piecewise-linear pressure) and (3) Q_2Q_{-1}, (same as Q_2P_{-1} except pressure is piecewise-bilinear). Even though the first and third have some (div-) stability problems [3], they produced excellent results and are still quite useful in general. The Q_2P_{-1} (9/3) element, while possibly the most popular higher-order element extant (at least when using quadrilaterals), was often less accurate than Q_2Q_{-1}. This may be more important in 3D simulations, where neither of these higher-order elements has been adaquately tested/evaluated. Some[3] suspect that Q_2Q_{-1}, even though somewhat unstable, may be the winner in this race.

The results presented in Tables 1-3 are self-explanatory, with the possible need to explain one 'outlyer': The Q_2P_{-1} element performed poorly (low amplitudes) on Mesh 1, but recovered strongly on Mesh 2. A final caveat: All results herein were at very slightly different parameter values; Ra ~ 3.41×10^5 and Pr ~ 0.709. The correct values will be used prior to the conference, and reported there.

Figure 1 gives the time history of the temperature at Point 1 for Q_2Q_{-1} on Mesh 2. Figure 1a focuses on the developing time regime, showing the frequency beating during the early stages that gives way to a single frequency. Figure 1b shows the single frequency behavior at later times in the solution. Figure 2 shows the pattern of temperature variations with respect to the local time average. The dark regions have an instantaneous temperature less than the local mean while in the gray regions it is greater. The arrows track a single disturbance 'bubble' over one oscillation period as it propagates up the hot wall.

In addition to those in the tables, we report briefly a few more results:

(1) The following elements failed totally (i.e., they went to a steady, non-oscillating flow state).

(i) Q_1Q_0 on meshes 1 & 2 when streamline upwinding was employed. (Not a surprise, considering that the fluid dynamical *instability* is in the boundary layer *in the flow direction.*)

(ii) Q_1Q_0 on mesh 1 using mass lumping, caused by poor phase speed accuracy (and inaccurate group velocity).

(iii) Q_2Q_1 (pressure is bilinear *continuous*) on mesh 1; also not a surprise – see Ref. 3.

(iv) Backward Euler for Q_1Q_0 on Mesh 1 using the same Δt that succeeded for TR (~25 steps/period).

3. The(less-expensive) advective form (e.g., $\mathbf{u}.\nabla\ \Theta$) was generally more accurate than either the conservation form [e.g.. $\nabla.(\mathbf{u}\Theta)$] or a quadratically-conserving (skew-symmetic) form— an average of the first two.

4. Q_1Q_0 seems to converge 'from above'; e.g.., the amplitudes of the oscillations are too large, whereas all three 'Q_2' elements seem to mostly converge from below—and, of course, faster.

5. References

[1] Christon, M.A., Gresho, P.M. Sutton, S.B., Special Session: Computationl predictability of natural conection flows in enclosures, First M.I.T. Conference on Computational Fluid andSolid Mechanics, M.I.T., Cambridge, Massachussets, U.S.A., June 12-14, 2001.

[2] FIDAP 8.52, Theory Manual, Fluent, Inc, Lebanon, N.H. Dec. 1999

[3] Gresho, P, and R. Sani, "Incompressible Flow and the Finite Element Method," J. Wiley & Sons, Chichester, 2000.

This work was performed under the auspices of the U.S. Department of Energy by the University of California, Lawrence Livermore National Laboratory under Contract No. W-7405-Eng-48.

Table 1; Point 1 Data

		Mesh 1 Grid resolution: 27x121 Steps / period: ~25			**Mesh 2** Grid resolution: 53x241 Steps / period: ~25			**Mesh 3** Grid resolution: 105x481 Steps / period: ~25		
		Avg.	Amp.	Period	Avg.	Amp.	Period	Avg.	Amp.	Period
u_1	Q_1Q_0	.05605	.02926	3.4583	.05861	.02822	3.4341	.05605	.02785	3.4279
	Q_2P_{-1}	.05246	.00271	3.4245	.05703	.02765	3.4265	.05665	.02774	3.4259
	Q_2Q_{-1}	.05601	.02597	3.4285	.05688	.02782	3.4261	.05554	.02774	3.4259
v_1	Q_1Q_0	.46189	.04123	3.4582	.4651	.03969	3.4342	.46163	.03915	3.4279
	Q_2P_{-1}	.46409	.00420	3.4428	.4631	.03877	3.4265	.46251	.03900	3.4259
	Q_2Q_{-1}	.46233	.03658	3.4285	.4627	.03912	3.4261	.46074	.03900	3.4259
Θ_1	Q_1Q_0	.26385	.02291	3.4582	.2664	.02197	3.4341	.26482	.02166	3.4279
	Q_2P_{-1}	.26590	.00221	3.4429	.2658	.02144	3.4265	.26547	.02156	3.4259
	Q_2Q_{-1}	.26590	.02025	3.4286	.2651	.02162	3.4261	.26468	.02158	3.4259
ε_{12}	Q_1Q_0	0	-	-	0	-	-	0	-	-
	Q_2P_{-1}	0	-	-	0	-	-	0	-	-
	Q_2Q_{-1}	0	-	-	0	-	-	0	-	-
ψ_1	Q_1Q_0	-.07293	.00369	3.4582	-.07397	.00360	3.4341	-.07450	.00356	3.4276
	Q_2P_{-1}	-.07337	.00035	3.4414	-.07398	.00353	3.4264	-.07444	.00354	3.4259
	Q_2Q_{-1}	-.07218	.00311	3.4286	-.07409	.00355	3.4261	-.07439	.00355	3.4259
ω_1	Q_1Q_0	-2.2379	.5764	3.4581	-2.3428	.5399	3.4341	-2.4144	.5388	3.4279
	Q_2P_{-1}	-2.4106	.0536	3.4414	-2.4240	.5431	3.4266	-2.4498	.5408	3.4259
	Q_2Q_{-1}	-2.2513	.5132	3.4285	-2.4190	.5465	3.4257	-2.4455	.5405	3.4259
ΔP_{14}	Q_1Q_0	-.00152	.01043	3.4582	-.00193	.01045	3.4340	-.00326	.01033	3.4280
	Q_2P_{-1}	-.00182	.00113	3.4412	-.00125	.01040	3.4264	-.00219	.01034	3.4262
	Q_2Q_{-1}	-.00135	.00987	3.4285	-.00200	.01048	3.4259	-.00203	.01034	3.4259
ΔP_{51}	Q_1Q_0	-.5337	.01119	3.4582	-.5332	.01150	3.4343	-.5323	.01146	3.4280
	Q_2P_{-1}	-.5342	.00131	3.4414	-.5348	.01149	3.4266	-.5348	.01146	3.4262
	Q_2Q_{-1}	-.5360	.01086	3.4286	-.5338	.01157	3.4260	-.5349	.01146	3.4260
ΔP_{35}	Q_1Q_0	.5362	.00505	3.4581	.5354	.00513	3.4341	.5357	.00510	3.4283
	Q_2P_{-1}	.5360	.00060	3.4422	.5360	.00513	3.4266	.5370	.00511	3.4261
	Q_2Q_{-1}	.5373	.00491	3.4286	.5358	.00517	3.4261	.5370	.00510	3.4257

Table 2; Nusselt Numbers

		Mesh 1 Grid resolution: 27x121 Steps / period: ~25			**Mesh 2** Grid resolution: 53x241 Steps / period: ~25			**Mesh 2** Grid resolution: 105x481 Steps / period: ~25		
		Avg.	Amp.	Period	Avg.	Amp.	Period	Avg.	Amp.	Period
$-Nu_{x=0}$	Q_1Q_0	4.5661	3.88e-3	3.4582	4.5796	3.70e-3	3.4343	4.5821	3.63e-3	3.4279
	Q_2P_{-1}	4.6318	4.30e-4	3.4410	4.5893	3.62e-3	3.4265	4.5825	3.61e-3	3.4259
	Q_2Q_{-1}	4.6328	3.70e-3	3.4286	4.5893	3.65e-3	3.4260	4.5821	3.61e-3	3.4258
$-Nu_{x=W}$	Q_1Q_0	4.5661	3.88e-3	3.4582	4.5796	3.70e-3	3.4343	4.5821	3.63e-3	3.4263
	Q_2P_{-1}	4.6318	4.39e-4	3.4421	4.5888	3.62e-3	3.4265	4.5825	3.61e-3	3.4259
	Q_2Q_{-1}	4.6328	3.70e-3	3.4286	4.5893	3.65e-3	3.4261	4.5821	3.61e-3	3.4258

Table 3; Mean Quantities

		Mesh 1 Grid resolution: 27x121 Steps / period: ~25			**Mesh 2** Grid resolution: 53x241 Steps / period: ~25			**Mesh 2** Grid resolution: 105x481 Steps / period: ~25		
		Avg.	Amp.	Period	Avg.	Amp.	Period	Avg.	Amp.	Period
$\hat{u}$	Q_1Q_0	.2396	2.21e-5	3.4582	.2396	1.78e-5	3.4335	.2397	1.73e-5	3.4271
	Q_2P_{-1}	.2393	2.99e-6	3.4336	.2397	1.69e-5	3.4265	.2397	1.71e-5	3.4254
	Q_2Q_{-1}	.2396	1.817e-5	3.4286	.2397	1.69e-5	3.4250	.2397	1.70e-5	3.4271
$\hat{\omega}$	Q_1Q_0	2.8728	.00155	3.4582	2.9769	.00160	3.4342	3.0075	.00161	3.4280
	Q_2P_{-1}	3.0188	.00019	3.4419	3.0180	.00161	3.4275	3.0179	.00161	3.4258
	Q_2Q_{-1}	3.0171	.00153	3.4285	3.0180	.00162	3.4260	3.0179	.00161	3.4259

Figure 1. The temperature at Point 1. (a) the early stages of flow development showing the frequency beating. (b) the latter stages of the solution, after stabilization, showing single frequency behavior.

Figure 2. Patterns of the instantaneous temperature variation from the local time averaged mean; time interval between plots is (approximately) 1/6 of one period. In dark regions the temperature is less than the local mean, in gray regions it is greater.

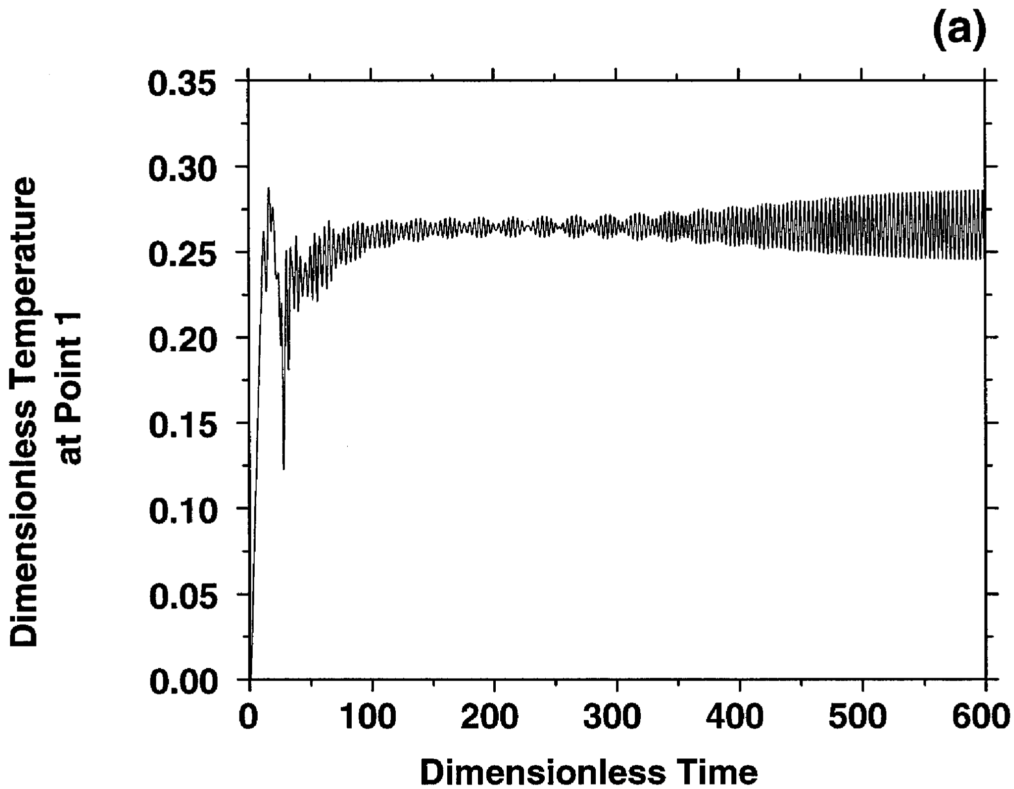
(a)
0.35
0.30
0.25
0.20
0.15
0.10
0.05
0.00
0
100
200
300
400
500
600
Dimensionless Time
Dimensionless Temperature
at Point 1

Figure 1a

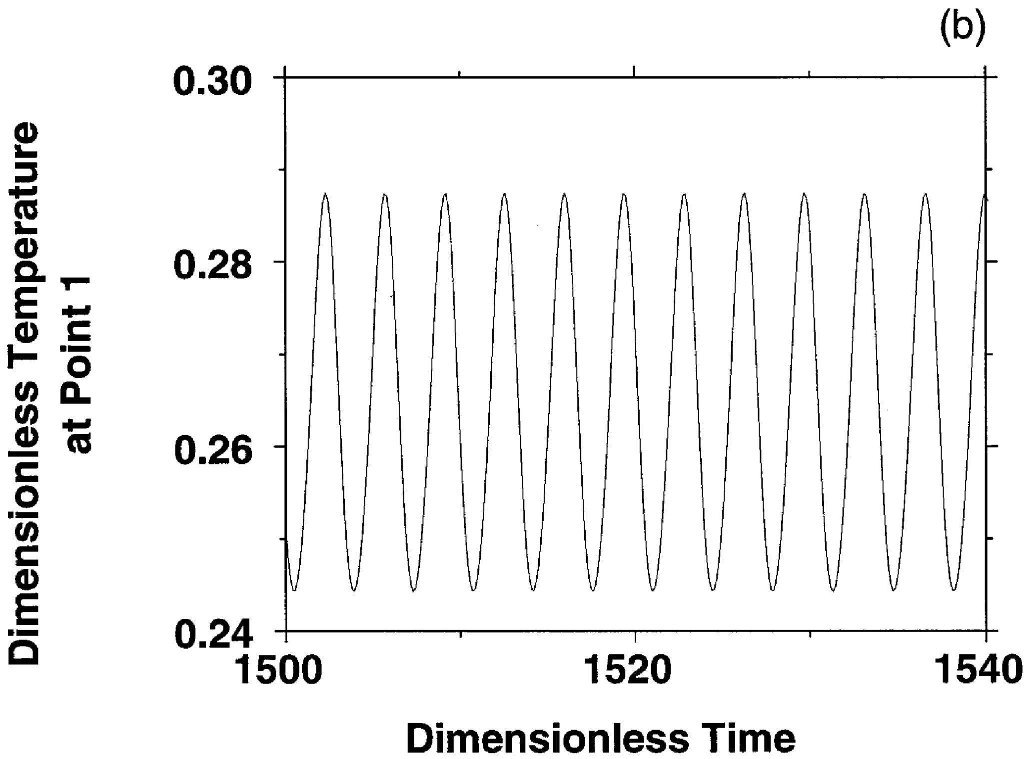
(b)
0.30
0.28
0.26
0.24
1500
1520
1540
Dimensionless Temperature at Point 1
Dimensionless Time

Figure 1b

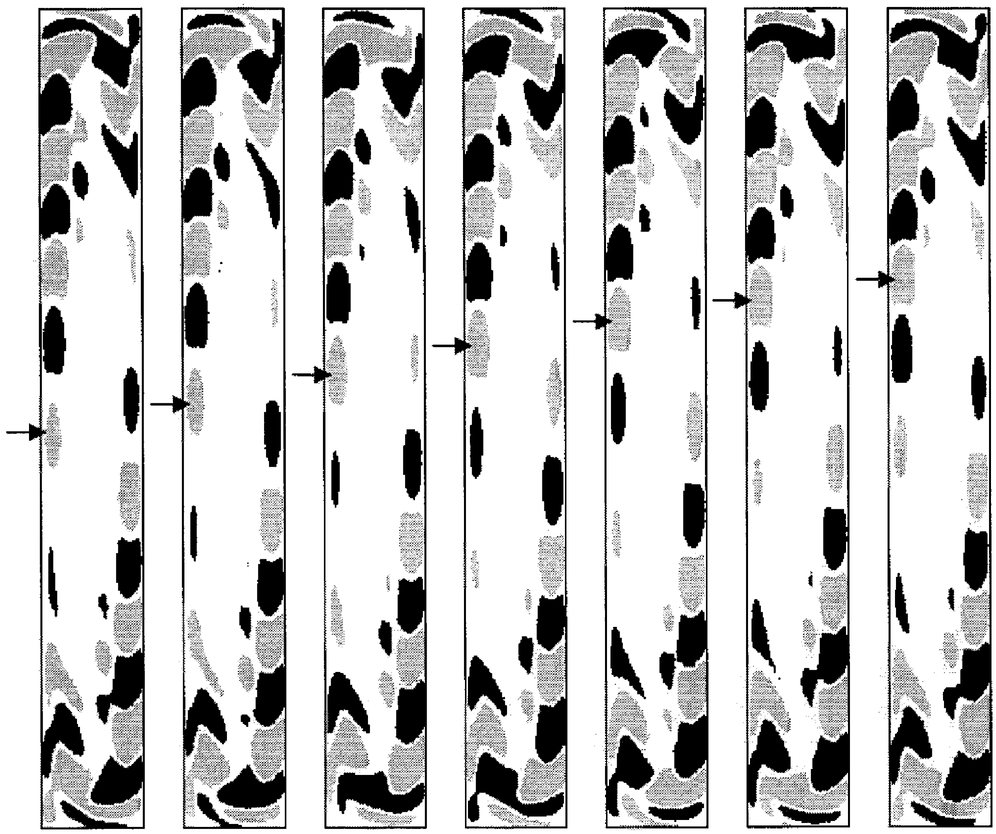

Figure 2

University of California
Lawrence Livermore National Laboratory
Technical Information Department
Livermore, CA 94551